

Test of the predictability of PI method on the Tohoku M_w 9.0 earthquake

*Yongxian Zhang¹, Cheng Song², Caiyun Xia³, Shengfeng Zhang⁴

1. China Earthquake Networks Center, 2. Institute of Earthquake Science, China Earthquake Administration, 3. Liaoning Earthquake Administration, 4. Institute of Geophysics, China Earthquake Administration

In this research, the local area (32.0°~46.0°N, 136.0°~148.0°E) including most of Japan was chosen to be the study region for verifying the predictability of the pattern informatics (PI) method under different models with different parameters using the receiver-operating characteristic (ROC) curve test and R score test. Pattern Informatics (PI) method was applied to the retrospective study on the forecasting of large earthquakes especially the Tohoku M_w 9.0 earthquake in this region. Different forecasting maps with different calculating parameters were obtained. The main calculating parameters were respectively the grid size of 0.5°×0.5° or 1.0°×1.0° and forecasting window lengths from 5 to 10 years. The results showed that in most of the models, the hotspots were in its Moore neighborhood grids or its epicentral grid in the forecasting windows containing the M_w 9.0 Tohoku earthquake, which suggests that the PI method could forecast the Tohoku M_w 9.0 earthquake. The results also showed that under the ROC test and R score test the models with larger grid size (1.0°×1.0°) and longer forecasting window length (7~10 years), the forecasting effect were better.

Keywords: PI method, Tohoku M_w 9.0 earthquake, predictability, ROC test, R score test

Nowcasting Global Earthquakes

*John B Rundle¹, Molly Luginbuhl¹, Alexis Giguere¹, Donald L Turcotte²

1. Department of Physics, University of California, Davis, California, USA 95616, 2. Department of Earth and Planetary Science, University of California, Davis, California, USA 95616

The term "nowcasting" refers to the estimation of the current uncertain state of a dynamical system, whereas "forecasting" is a calculation of probabilities of future state(s). Nowcasting is a term that originated in economics and finance, referring to the process of determining the uncertain state of the economy or markets at the current time by indirect means.

We have applied this idea to seismically active regions, where the goal is to determine the current state of a system of faults, and its current level of progress through the earthquake cycle

(<http://onlinelibrary.wiley.com/doi/10.1002/2016EA000185/full>).

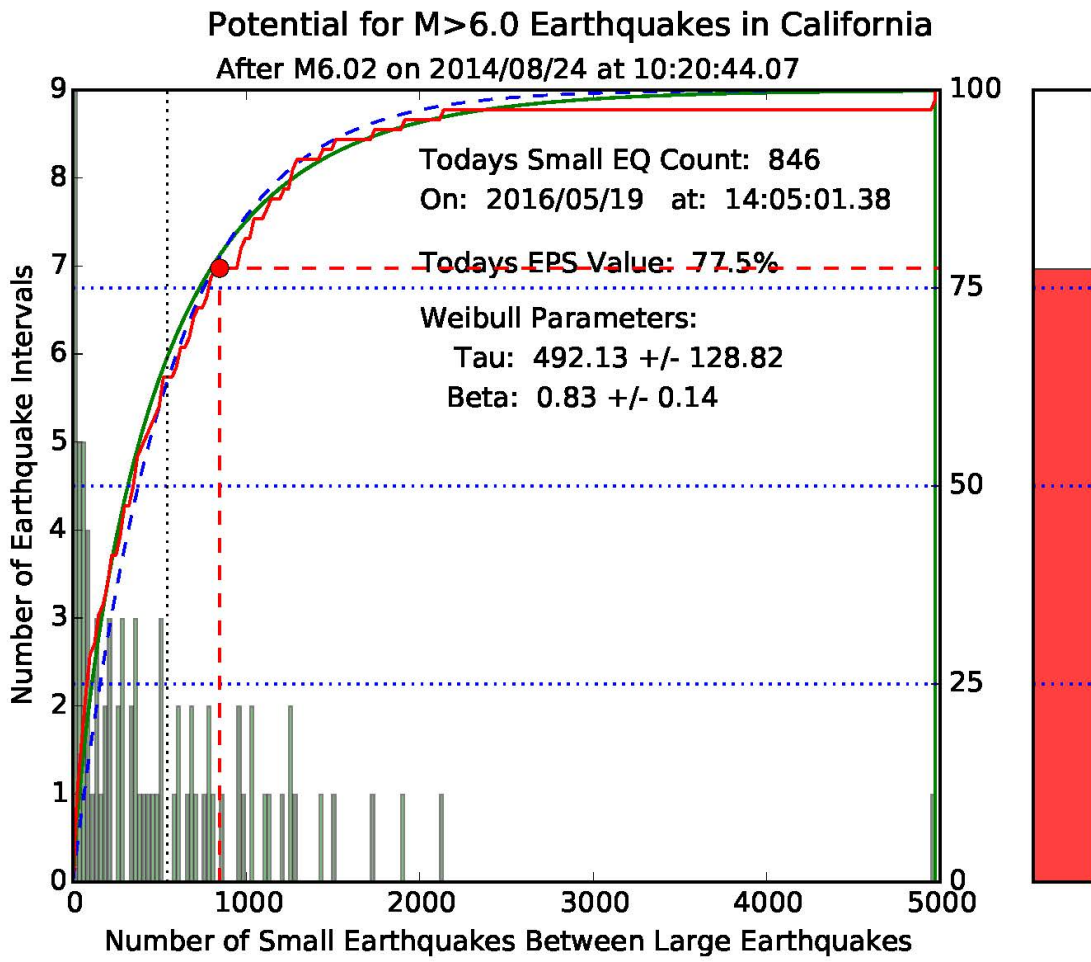
We wish to estimate how far the fault system has progressed through the "cycle" of large recurring earthquakes. We use the global catalog of earthquakes, using "small" earthquakes to determine the level of hazard from "large" earthquakes in the region. As an application, we can define a small region around major global cities, for example a "small" circle of radius 150 km and a depth of 100 km, as well as a "large" earthquake magnitude, for example M6.0. Also, the region of influence of such earthquakes is roughly 150 km radius x 100 km depth, which is the reason these values were selected.

The statistics are computed from a "large" $10^\circ \times 10^\circ$ region surrounding the "small" 150 x 100 km circle. The current count of earthquakes that is used to compute the nowcast is obtained from small earthquakes in the small region. The basic assumption is that both the "large" and "small" regions are characterized by the same Gutenberg-Richter magnitude frequency statistics.

If one defines a "model" as a calculation system in which there exist free parameters that must be optimally fit to data, then it can be said that there is no model involved in our nowcasting analysis. Our methods involve only plotting and interpreting data, once the magnitude threshold and spatial region have been selected.

We have used these techniques to compute the relative nowcast rankings of large global cities at risk for damaging earthquakes. In this talk we discuss these rankings. We also discuss the results of sensitivity analyses of the rankings to variations in the selected magnitude, small and large regions.

Keywords: Global Earthquakes, Nowcasting, Sensitivity testing



Detailed inversion of a shallow slow slip event at the Hikurangi subduction zone, New Zealand, using numerical Green's functions and absolute pressure gauge data

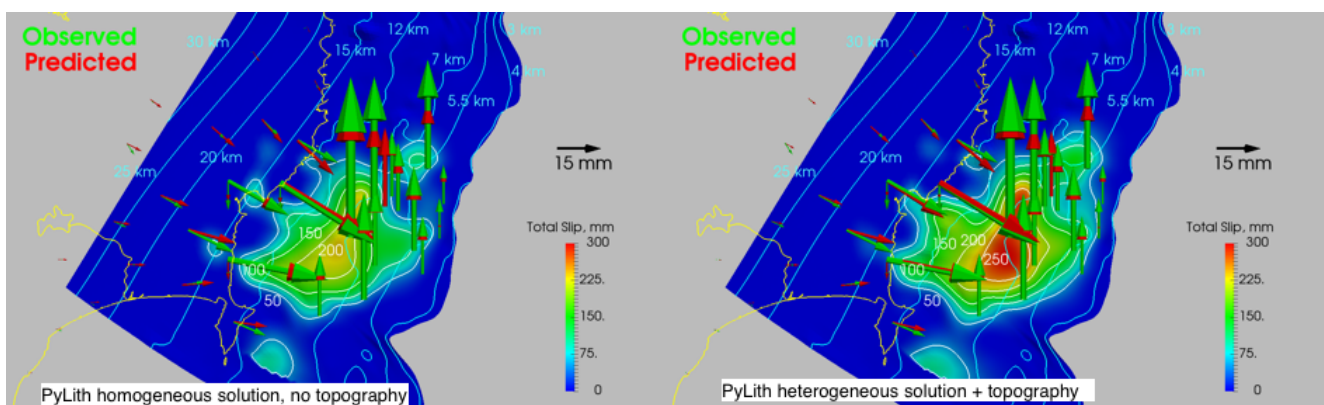
*Charles A Williams¹, Laura M Wallace¹, Spahr C Webb², Yoshihiro Ito³, Kimihiro Mochizuki⁴, Ryota Hino⁵, Stuart Henrys¹

1. GNS Science, 2. Lamont-Doherty Earth Observatory, 3. Disaster Prevention Research Institute, 4. Earthquake Research Institute, 5. Tohoku University

Slow slip events (SSEs) have been observed throughout the world, and the existence of these events has fundamentally altered our understanding of the possible ranges of slip behavior at subduction plate boundaries. SSEs are typically observed via continuous GPS (cGPS) observations. Although much has been learned in recent years, the slip distributions for shallow SSEs are still poorly understood due to the lack of offshore data to constrain the slip estimates. Most importantly, it has been difficult to determine whether shallow SSEs extend to the trench, or whether they terminate at some distance inboard of the trench. Constraining the slip distribution is critical to our understanding of the physics underlying SSEs.

Recently, absolute pressure gauges (APGs) were deployed offshore near Gisborne, New Zealand, as part of the HOBITSS experiment, capturing a SSE event during September and October 2014. The APGs provide a record of vertical deformation during the event, allowing much better constraints on the offshore slip distribution. Initial inversions using an elastic half-space model based on these observations indicate that slip occurred within 2 km of the trench. We here describe a more detailed inversion procedure where we include the effects of detailed fault geometry, bathymetry/topography, and material property variations to provide a more accurate estimate of the slip distribution during this event. We use the PyLith finite element code to generate Green's functions for use in our inversions. We find that inversions that take into account material property variations require larger amounts of slip, with predicted seismic potencies approximately 40% greater than homogeneous models.

Keywords: Slow slip, Hikurangi, Inversion, Numerical Green's functions, Absolute pressure gauge, Finite element



The 12 September 2016 M_L 5.8 Gyeongju, Korea, earthquake: Observation and questions

*Tae-Seob Kang¹, Kwang-Hee Kim², Junkee Rhie³, Younghee Kim³

1. Division of Earth Environmental System Science, Pukyong National University, 2. Department of Geological Science, Pusan National University, 3. School of Earth and Environmental Sciences, Seoul National University

The M_L 5.8 earthquake in Gyeongju, southeastern Korea, on September 12, 2016 11:32:54 (UTC) was the largest earthquake on the Korean Peninsula since instrumental monitoring began in 1978. It was preceded by an M_L 5.1 foreshock and is being followed by numerous aftershocks. Within an hour of the mainshock, the first temporary seismic station to monitor aftershocks was installed at about 1.5 km east of the announced epicenter. The temporary seismic network consists of 27 stations equipped with broadband sensors covering an area of about 38 x 32 km² in the mainshock region. This is the first high-density aftershock monitoring array in the Korean Peninsula. Initial results, using data from both the regional seismic networks and the aftershock monitoring array, indicate that earthquakes during the first 10 days following the mainshock are related to the Yangsan Fault System. The 2016 Gyeongju events have now become forceful reminders that earthquakes have occurred in the past and can hit the region again at any time. These earthquakes provide an opportunity to reaffirm aspects already known based on evidence from both historical (literature) and seismological data. Moreover, the occurrence of the 2016 Gyeongju earthquakes has motivated more detailed studies of the Yangsan Fault System and a reexamination of the previously held consensus regarding the fault system. The most frequently asked questions during the Gyeongju earthquake crisis are as follows: Are there any active faults in the source area? Which faults are responsible for the mainshock–aftershock sequence? Is the Yangsan fault active? Is it possible to release information regarding impending earthquake activity? How long will the aftershocks continue? What is the next earthquake scenario and how to model it? These issues will be discussed on the basis of the aftershock monitoring data.

Keywords: Gyeongju, Korea, earthquake, responsible fault, future earthquake scenario

Dynamic Faulting Simulation with Cellular Automaton Model

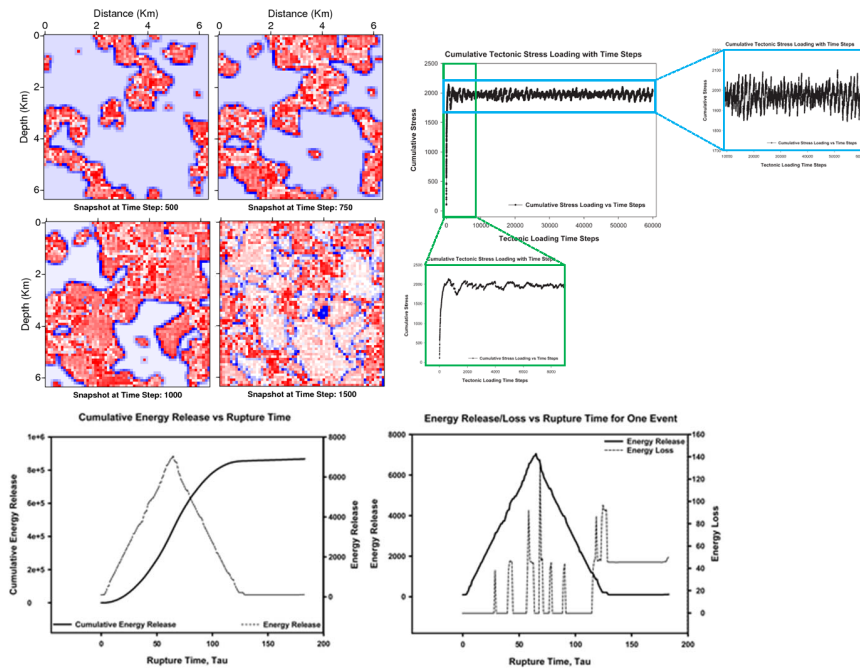
*How-wei Chen¹

1. Institute of Geophysics, National Central University, Taiwan, ROC

Earthquake dynamics are believed to exhibit self-organized criticality (SOC). The apparent unrest of dynamic stress changes of the crust to stress perturbations exhibits similar SOC behavior. Cellular Automaton Model (CAM) is implemented in simulating dynamic faulting processes. Early stage investigation aims in probing system dynamics by seeking any available simulation schemes including granular material, lattice-gas and lattice-solid approaches. The simulation can be realized through iterative application of rules that encapsulate the essential physics of the system by allowing uniform stress increment but rupture can be initiated and re-distributed fractally depends on the pre-defined rock strength. Automata rules control the stress concentrations that form ahead of growing ruptures and can be physically justified by assuming that failed cells have not yet healed and thus cannot support stress. We assume ruptures occur instantaneously under two distinct timescales - tectonic loading and rupture timescales. The occurrence of the faulting/fracturing can be modeled base on the dispassion (relaxation) factor and stress transfer ratio that controls the onset of instability and size of nucleation zone. Only fractional part of stress on the failing cell is redistributed to mimic dissipation where energy is lost for fracture opening, generation of seismic waves and heat generation. CAMs allow cells and eight nearest neighbors to fail repeatedly or only fail once in a single event. The event size corresponds to the total number of cells failed in a single step. The heterogeneous automaton allows redistributes stress to the unbroken nearest neighbors and hence produce more realistic stress concentrations. A Large event can be initiated from many small ones which expand as the result of interactions between tectonic loading, stress concentration, growing of rupture-front, broken or unbroken cells and local variations in fault strength. The distribution of rock strength can be homogeneous, random or fractal. No additional increment of stress is added until after rupture has ended. Spatial and temporal power-laws which statistically exhibit magnitude-frequency (size-number) distributions can be analysis from synthesized earthquake catalogs. More complex fault models to describe the geometry of nature faults can be characterized by fractal statistics with different scales.

CAM simulation encapsulates the essential physics of the system. The apparent sensitivity of crust to small stress perturbations and the occurrence of triggered earthquakes suggest that the Earth's crust behaves similarly critical. The distribution of rock strength can be homogeneous, random or fractal. The faults are zones of weakness within the crust and individual faults may have strength fluctuations due to short-range, local variations in pore pressure and surface roughness. Alternatively, long-range elastic/visco-elastic interactions can be incorporated as well. The fault strength with surface roughness can be described with fractal dimension of 2.3. The accumulated stress is distributed to its eight surrounding neighbors with the pre-defined dispassion factor and stress transfer ratio. Tectonic loading can be uniform, random or fractal too. Cellular automaton models allow cells and eight nearest neighbors to fail repeatedly or only fail once in a single event. The heterogeneous automaton allows redistributes stress to the unbroken nearest neighbors and hence produce more realistic stress concentrations. Automata rules control the stress concentrations that form ahead of growing ruptures and can be physically justified by assuming that failed cells have not yet healed and thus cannot support stress. Only 75% of stress on the failing cell is redistributed to mimic dissipation (relaxation) where energy is lost to seismic waves and heat generation.

Keywords: Cellular automaton, lattice solid, dynamic rupture, numerical modeling, instability, self-organized criticality (SOC)



Conceptual Model for Precursory Slow Slip and Foreshocks based on the Balance of Stiffness on and around the Fault

*Eiichi Fukuyama¹, Futoshi Yamashita¹, Shiqing Xu¹, Shigeru Takizawa¹, Kazuo Mizoguchi^{1,2}, Hironori Kawakata^{1,3}

1. National Research Institute for Earth Science and Disaster Prevention, 2. Central Research Institute of Electric Power Industry, 3. Ristumeikan University

We propose a conceptual model to understand the occurrence of precursory slow slip and foreshocks, both of which may occur prior to the mainshock. First, we summarize our experimental results of large-scale bi-axial shear friction experiments using the NIED large-scale shaking table (e.g. Fukuyama et al., 2014, Yamashita et al., 2015). In a series of experiments using an Indian metagabbro sample whose nominal slip area was 1.5m long and 0.1m wide, precursory slow slip events occurred in most cases but foreshocks were only observed under certain conditions related to the fault surface damage. When foreshocks occurred, they initiated inside the slow slip area and both coexisted. In addition, from the hypocenter distribution of foreshocks and the observation of the fault damage evolution, foreshocks tend to be initiated at the edge of grooves on the fault surface. To understand the observation described above, we shall follow the idea of Leeman et al. (2016) and Kilgore et al (2017), where the balance between the stiffness of the apparatus and that of fault surface controls. Leeman et al. (2016) varied the fault stiffness by changing the amount of normal stress while Kilgore et al (2017) varied the apparatus stiffness using springs with different elastic constants. The evolution of fault damages could be related to the apparent change in the b-a value in rate- and state- dependent friction regime (Beeler et al., 1996, Urata et al., 2016). As fault damage evolves, apparent b-a value increases. Under steady state conditions, b-a value is proportional to the fault stiffness (if positive). And we could assume that the apparatus stiffness remain constant during the episodes. Therefore, we could say that slow slip occurs where the fault stiffness is smaller than the apparatus stiffness and foreshocks occur where the fault stiffness is larger than the apparatus stiffness. In addition, Yamashita et al (2015) showed a heterogeneous distribution of local normal stress on the fault surface, especially around the grooves, and Leeman et al. (2016) showed that normal stress is also proportional to the fault stiffness. These heterogeneous distributions of normal stress and friction parameters may also cause a coexistence of slow slip and foreshocks, since the groove distribution is not uniform on the fault. In nature, stiffness of the apparatus corresponds to the stiffness of the surrounding materials of the fault. Precursory slow slip events and foreshocks can be understood based on the differences in stiffness of the fault and surrounding materials.

References:

- Beeler et al. (1996) *J. Geophys. Res.*, doi:10.1029/96JB00411
Fukuyama et al. (2014) NIED Report, http://dil-opac.bosai.go.jp/publication/nied_report/PDF/81/81-3fukuyama.pdf
Kilgore et al (2017) AGU Monograph, in press.
Leeman et al. (2016) *Nature Comm.*, doi:10.1038/ncomms11104
Urata et al. (2016) *Pure Appl. Geophys.*, doi:10.1007/s00024-016-1422-9
Yamashita, et al. (2015) *Nature*, doi:10.1038/nature16138

Keywords: Slow slip, Foreshock

Comparison of the initial rupture processes between the M_w 6.2 mainshock and the M_w 4.1 largest foreshock of the central Tottori earthquake on October 21, 2016

*Shunta Noda¹, William L. Ellsworth²

1. Railway Technical Research Institute, 2. Stanford University

It is one of the essential questions in seismology whether or not the rupture termination of an earthquake is deterministic at the time of initiation (e.g., Iio, 2009). To investigate this issue, Noda and Ellsworth (2016, GRL) statistically characterized initial P waves using Japanese K-NET dataset. They concluded that the P-wave displacement began in a similar way at the onset and departed from the similarity earlier for smaller events in the magnitude range up to M_w 7. The departure time (T_{dp}) is approximately 30% of typical source duration, implying a connection between initial rupture process and the final earthquake size. To discuss this, we model slip histories during the initial stages of the M_w 6.2 central Tottori earthquake on October 21, 2016 in Japan and its largest foreshock of M_w 4.1 that occurred about two hours before the mainshock. Because these hypocenters are co-located and the focal mechanisms are identical according to the JMA catalog, we invert them using the same empirical Green's functions derived from other foreshocks. We use the Hi-net records surrounding the hypocenters and solve a linear system defined by the representation theorem for seismic sources using non-negative least squares method (Lawson and Hanson, 1974). Our result demonstrates that both ruptures initiate in a similar way until approximately 0.2 s after the nucleations. For the foreshock, the rapid growth completes at about 0.2 s which is consistent with T_{dp} and the duration of the "growth stage" (Uchide and Ide, 2010). On the other hand, for the mainshock, it continues to grow up rapidly even after 0.2 s. We consider that this variation in initiating process may have resulted in the difference of the final sizes.

Keywords: Initial rupture, Nucleation, The 2016 central Tottori earthquake, Slip inversion, Kinematic modeling, Deterministic property

Simultaneous estimation of the dip angles and slip distribution on the two active faults of the 2016 Kumamoto earthquake

*Yukitoshi Fukahata¹, Manabu Hashimoto¹

1. Disaster Prevention Research Institute, Kyoto University

At the 2016 Kumamoto earthquake, surface ruptures were observed not only along the Futagawa fault, where main ruptures occurred, but also along the Hinagu fault. To estimate the slip distribution on these faults, we extend a method of non-linear inversion analysis (Fukahata and Wright 2008) to a two-faults system. With the method of Fukahata and Wright (2008) we can simultaneously determine the optimal dip angle of a fault and the slip distribution on it, based on Akaike's Bayesian Information Criterion (ABIC) by regarding the dip angle as an hyperparameter. By inverting the InSAR data with the developed method, we obtain the dip angles of the Futagawa and Hinagu faults as $61^\circ \pm 6^\circ$ and $74^\circ \pm 12^\circ$, respectively. The slip on the Futagawa fault is mainly strike slip. The largest slip on it is over 5 m around the center of the model fault (130.9° in longitude) with a significant normal slip component. The slip on the Futagawa fault quickly decreases to zero beyond the intersection with the Hinagu fault. On the other hand, the slip has a local peak just inside Aso caldera, which would be a cause of severe damage in this area. A relatively larger reverse fault slip component on a deeper part around the intersection with Aso caldera suggests that something complicated happened there. The slip on the Hinagu fault is almost a pure strike slip with a peak of about 2.4 m. The developed method is useful in clarifying the slip distribution, when a complicated rupture like the Kumamoto earthquake happens in a remote area.

Keywords: The 2016 Kumamoto earthquake, weak nonlinear inversion analysis, ABIC

Rupture processes of the 2016 Kumamoto earthquake sequence: Causes for extreme ground motions

*Hiroaki Kobayashi¹, Kazuki Koketsu¹, Hiroe Miyake^{2,1}

1. Earthquake Research Institute, The University of Tokyo, 2. Interfaculty Initiative in Information Studies, The University of Tokyo

The 2016 Kumamoto earthquake sequence including three large events (M6.5 on April 14, M6.4 on April 15, and M7.3 on April 16) caused severe damage to the Kumamoto prefecture and surrounding region. During the M7.3 event, extreme pulse-like velocity waveforms were observed in the town of Mashiki and the village of Nishihara. To investigate the rupture processes of the 2016 Kumamoto earthquake sequence and causes for these pulse-like waveforms, we performed the joint source inversions of the three notable events using strong motion, teleseismic, and geodetic data.

We constructed multi-segment faults models for the three events. We first relocated the hypocenters of the sequence by double difference method [Waldhauser and Ellsworth, 2000]. Considering the relocated hypocenters distributions, focal mechanisms, and active faults, we divided the source region into four regions. Four regions correspond to the Hinagu fault zone, the junction of the Futagawa and Hinagu fault zones, the Futagawa fault zone, and the inner Aso caldera. We also adjusted the one-dimensional velocity structure models for strong motion stations using five medium-sized earthquakes.

The obtained results are following: 1) The M6.5 event initiated on southeast dipping fault and then ruptured the Hinagu fault toward southwest; 2) The M6.4 event initiated on the Hinagu fault and ruptured the adjacent region to the M6.5 rupture area; 3) The M7.3 event initiated on the deep part of the Hinagu fault and propagate to northeast along the Futagawa fault; 4) Extreme ground motion observed in the town of Mashiki and the village of Nishihara can be attributed to the event's upward rupture directivity and fast slip rate.

Keywords: 2016 Kumamoto earthquake, rupture process, joint inversion

Dynamic rupture simulation of two cascading foreshocks of the 2016 Kumamoto earthquake

*Hiroki Arai¹, Ryosuke Ando², Yosuke Aoki³

1. Faculty of Science, University of Tokyo, 2. Graduate School of Science, University of Tokyo, 3. Earthquake Research Institute, University of Tokyo

The 2016 Kumamoto earthquake sequence, including two major foreshocks (Mw 6.2 and 6.0) and the main shock (Mw 7.0), hit the Kyushu island of southwest Japan. The foreshocks have a temporal separation of approximately 2.5 hours; the latter one has apparently been triggered by the former one by its change in static stress, dynamic stress, or both. We assumed that those foreshocks had ruptured subparallel but different faults on the Hinagu fault system, and constructed a dynamic model to gain insights into the mechanism of such consecutive events by computing the temporal evolution of stress and slip rate on both faults using Boundary Integral Equation Method. Our results show that, under circumstances satisfying local stress field constrained by an independent information of spatial variations of earthquake focal mechanisms, the rupture of former foreshock dynamically triggered the second foreshock. In addition, parameter studies gave us indication of the relationship between local frictional properties and stress field. Our result is also consistent with observed ground deformation from the ALOS-2 Synthetic Aperture Radar satellite.

Keywords: Dynamic rupture simulation, Kumamoto Earthquake, Synthetic Aperture Radar

3-D Dynamic Rupture Simulations of the 2016 Kumamoto, Japan, Earthquake

*Yumi Urata¹, Keisuke Yoshida², Eiichi Fukuyama¹

1. National Research Institute for Earth Science and Disaster Resilience, 2. Tohoku University

Using 3-D dynamic rupture simulations, we investigated the 2016 M7.3 Kumamoto, Japan, earthquake to illuminate why and how the rupture of the main shock propagated successfully, assuming a complicated fault geometry estimated on the basis of the distributions of the aftershocks. The M7.3 main shock occurred along the Futagawa and Hinagu faults. A few days before, three M6-class foreshocks occurred. Their hypocenters were located along the Hinagu and Futagawa faults, and their focal mechanisms were similar to those of the main shock; therefore, an extensive stress shadow may have been generated on the fault plane of the main shock. First, we estimated the geometry of the fault planes of the three foreshocks as well as that of the main shock based on the temporal evolution of the relocated aftershock hypocenters. We then evaluated the static stress changes on the main shock fault plane that were due to the occurrence of the three foreshocks, assuming elliptical cracks with constant stress drops on the estimated fault planes. The obtained static stress change distribution indicated that the hypocenter of the main shock was located in the region with a positive Coulomb failure stress change (Δ CFS), while the Δ CFS in the shallow region above the hypocenter was negative. Therefore, these foreshocks could encourage the initiation of the main shock rupture and could hinder the propagation of the rupture toward the shallow region. Finally, we conducted 3-D dynamic rupture simulations of the main shock using the initial stress distribution, which was the sum of the static stress changes caused by these foreshocks and the regional stress field. Assuming a slip-weakening law with uniform friction parameters, we conducted 3-D dynamic rupture simulations by varying the friction parameters and the values of the principal stresses. We obtained feasible parameter ranges that could reproduce the characteristic features of the main shock rupture revealed by seismic waveform analyses. We also demonstrated that the free surface encouraged the slip evolution of the main shock.

Dynamic rupture simulation with complex fault geometries for the 2016 Kaikoura, New Zealand, earthquake

*Ryosuke Ando¹, Yoshihiro Kaneko²

1. Graduate School of Science, University of Tokyo, 2. GNS Science

The 2016, Mw 7.8, Kaikoura earthquake is a unique event with its rupture process that propagated through the significantly complicated fault system, suggested according to field surveys and an Interferometric synthetic aperture radar InSAR observation (Hamling et al., 2017, submitted). The InSAR observation infers up to 19 fault segments, where some of them are newly identified. Since the fault geometry is considered as one of primary parameters controlling the initiation, propagation and termination of earthquake ruptures, it is important to understand which conditions allow the rupture to propagate through multiple fault segments having such complicated geometries. In this study, we apply the dynamic rupture simulation to reproduce the observed rupture processes and slip distributions. For the numerical analysis, we employ the spatio-temporal boundary integral equation method with the fast domain partitioning method (FDPM), which enables us the accurate and efficient analyses of the nonplanar fault geometry. The fault model is developed by referring Hamling et al. (2017). The regional stress field is determined based on the seismological stress tensor inversion done previously in this region (Balfour et al., 2005, GJI). The observationally constrained stress axes were consistent with the overall dextral faulting of the NE-SW trended fault systems but locally some fault segments appear to be obliquely oriented. The preliminary computation shows that the distribution of the tractions resolving the regional stress on each fault segment was largely varied over the fault system, suggesting to cause the complex rupture process.

Keywords: Dynamic rupture simulation, Boundary integral equation method, Complex fault geometry

Strain rate effect on rupture nucleation and mainshock propagation speed

*Shiqing Xu¹, Eiichi Fukuyama¹, Futoshi Yamashita¹, Kazuo Mizoguchi², Shigeru Takizawa¹, Hironori Kawakata³

1. NIED, Japan, 2. CRIEPI, Japan, 3. Ritsumeikan Univ.

Multiple lines of evidence have indicated that the same fault portion can host a diverse spectrum of deformation modes. They include the coexistence of pseudotachylite and mylonite near the base of the seismogenic zone, the coexistence of slow slip and unstable rupture in the Japan Trench as well as in the laboratory, and the transient deepening of seismicity below the normal brittle-to-ductile transition depth after a major earthquake. In addition to pressure-temperature condition and material composition, strain rate has been invoked to explain the diversity and switch of deformation modes of solids. In this work, we investigate how strain rate may affect the behavior of fault slip, based on direct shear experiments using meter-scale rock samples made of Indian metagabbro (nominal fault area is 1.5 m x 0.1 m). In addition to the macroscopic frictional behavior measured by load cells, we monitor the local fault behavior utilizing a high-density array of strain gauges mounted close to the synthetic fault (20-40 mm off the fault). We conduct experiments under a constant normal stress of 6.7 MPa, and a constant loading rate ranging from 0.01 mm/s to 1 mm/s. For the highest loading rate, we focus on the early part right after the initial running-in stage, during which fault surface condition has not been significantly altered. We approximately evaluate the strain rate by referring to the applied loading rate over a fixed sample size, while also point out that the actual local strain rate can greatly fluctuate depending on the ongoing deformation mode. Our macroscopic observation shows that for all the tested cases the fault motion is characterized by stick-slip, implying an overall brittle faulting regime. Detailed local observation reveals that quasi-stable slow slip phase preceding unstable mainshocks is a common feature for cases under a low loading rate (e.g. 0.01 mm/s), but can be skipped (below the 50-mm resolution of our strain gauge array) under a high loading rate (e.g. 1 mm/s). Another related local observation is that mainshock propagation speed is often faster under a higher loading rate, possibly exceeding the shear wave speed of metagabbro (i.e. supershear rupture). Based on the well-known theoretical result that the balance between elastic strain energy and fracture energy controls the critical transition length scales and rupture speed (Madariaga and Olsen, 2000), we suggest the following ideas for understanding our laboratory observations. (1) High-rate loading can more efficiently transfer energy to the rock bulk, and the average stress level operating over the entire fault can well exceed that set by the weakest fault patch. (2) High-rate loading can enhance the brittleness of fault rocks by reducing the apparent fracture energy (Freund, 1990): some inelastic process will not have enough time to dissipate energy before the failure criterion is reached near a rapidly stressed rupture front. It should be noted that the above point (2) is not always true, as in other circumstances high-rate loading can cause an increase in the apparent fracture energy through mechanisms such as rupture bifurcation, intense microcracking, and gouge generation. When these scenarios occur, rupture propagation may strongly fluctuate or even get arrested. Therefore, more investigations are needed to categorize strain rate effect during different stages of fault slip.

Keywords: Strain rate, Rupture nucleation, Mainshock propagation

Supershear rupture induced by step over geometry

*Feng Hu¹, Hengxin Ren², Xiaofei Chen^{1,2}

1. Univ. of Sci. &Tech. of China, 2. Srn. Univ. of Sci. & Tech.

Based on dynamic rupture simulations on strike-slip step overs in a 3-D full space where the initial shear stresses preclude a supershear transition according to the Burridge-Andrews supershear transition mechanism, we show that rupture speeds can transit from subshear on the primary fault to supershear on the secondary fault for both compressional and extensional step overs. The low normal stress zone and the high shear stress zone, which radiate from the end of the primary fault if its rupture arrest is sudden, coincides beyond the fault step, and determine the supershear rupture occurrence on the secondary fault. However, a low shear stress zone traveling at the shear wave speed is also radiated, making the rupture speed return to subshear in most cases. Sustained supershear rupture are also possible on compressional step overs under certain conditions. Self-arresting ruptures are observed in the overlap area on the secondary fault. In the homogeneous half-space model where supershear rupture exists on the primary fault, because of the free-surface, the rupture speed on the secondary fault rapidly transits to subshear near the fault step if its width exceeds a critical value. The distribution of peak ground velocities are also investigated.

Keywords: supershear ruptures can be induced by a fault step over, stress waves radiated from the end of the primary fault control supershear transition on secondary fault segments, rapid rupture speed transitions at step overs in a half-space

Synchronization of Stick-Slip Oscillator by Periodic External Forces -Elastic and Viscoelastic Cases-

*Kazuro Hirahara¹

1. Department of Geophysics, Earth and Planetary Sciences, Graduate School of Sciences, Kyoto University

In the last JpGu meeting, I reported the responses of stick-slip oscillator to periodic external forces. There, I examined the quasi-dynamic motion of a block connected with a spring pulling with a constant loading rate vpl , where the laboratory-derived rate- and state-friction law is working on the contact surface between the block and the underlying floor. I used frictional parameters a , b , L appropriate for velocity weakening and the spring constant k less than a critical stiffness k_c to produce a repeating stick-slip motion of the block, which is a simple earthquake cycle model with a recurrence time. Then, I applied periodic external forces with several periods and observed clear $m:n$ synchronization phenomena with synchronization frequency (period) widths, which is so called 'Devil's Staircase'. Here, $f_e:f_c$ ($T_c:T_e$)= $m:n$ (m and n are coprime integers) where f_e and f_c (T_c and T_e) are frequencies (periods) of the external force and the simulated system, respectively.

This paper is a continuation of the previous one. The $m:n$ synchronization is clear for the external force with the amplitude larger than 10 or 1 percent of stress drop during an earthquake cycle. At first, I supposed to use this synchronization for explaining the observed statistical significance of periodicity and seasonality of seismic activities. The stress changes of periodic daily and long-term tidal forces is an order of kPa. The amplitude of stress drop for usual earthquakes and slow slip events (SSEs) is an order of MPa and kPa. Then tidal forces can contribute to synchronization of SSEs, but not of usual earthquakes. But a simulation study shows a possible existence of long-term SSE with a larger stress drop of 0.1 MPa, which causes synchronization of large earthquakes such as those along the Nankai trough. The other extension is to investigate viscoelastic cases. The elastic spring is replaced by the standard linear solid, where the elastic spring with k_1 and the Maxwell viscoelastic element (a spring with k_2 is serially connected with a dash-pot of viscosity η) are connected in parallel, and the relaxation time is $\tau_r=k_2/\eta$. The change of relaxation time τ_r causes the recurrence times. And I discuss the synchronization in these viscoelastic cases, comparing with the elastic cases.

Keywords: Stick-Slip Oscillator, Synchronization, Rhythm, Earthquake Cycle Simulation, Periodic External Force, Elastic and Viscoelastic

Physics-based simulation for possible interplate earthquakes along the Nankai trough

*Chihiro Hashimoto¹, Yumi Urata², Eiichi Fukuyama²

1. Graduate School of Environmental Studies, Nagoya University, 2. National Research Institute for Earth Science and Disaster Resilience

In order to numerically generate possible earthquake scenarios for the Eurasian-Philippine Sea plate interface along the Nankai trough in southwest Japan, we need to assimilate diverse observation data into a physics-based 3-D model of earthquake generation cycles. Hashimoto *et al.* (2014) developed a numerical simulation system which consists of the quasi-static tectonic loading model and the dynamic rupture propagation model, based on the common 3-D model of plate interface geometry. In the theoretical framework of this system, our problem is to simulate time evolution of stress states so that the past slip history at plate interfaces estimated from observation data is adequately reproduced. Given the stress state and fault constitutive relation just before the earthquake occurrence, we can compute the subsequent rupture propagation process. In the numerical methods to reproduce realistic stress states and to generate possible earthquake scenarios, it is essential to assign a proper fault constitutive relation to control both the processes of quasi-static tectonic loading and dynamic rupture propagation. In the present study, we use the slip- and time-dependent fault constitutive law proposed by Aochi and Matsu'ura (2002), where time evolution of macroscopic relation between fault slip and shear strength is prescribed by the abrasion rate and the adhesion rate of microscopic fault surface topography and a constant representing mechanical properties of the contact zone, and therefore we need to examine distribution of these parameters. Interseismic increase rates of slip deficit along the Nankai trough inferred from GPS data inversion are used to constrain the constitutive parameters and to verify the numerical results. The sequence of the past large interplate earthquakes and their rupture initiation points and coseismic slip distributions are also used. Setting proper distribution of the constitutive parameters, we can generate possible earthquake scenarios with the method developed by Hok *et al.* (2011), which enables us to discuss potential earthquakes along the Nankai trough in terms of stress states at the moment and the relevant possible dynamic ruptures under inherent stress disturbances.

Sea-surface Displacement and Tsunami Inundation Including Seismic Waves and Tsunami for Anticipated Nankai Trough Earthquakes, Southwest, Japan

*Tatsuhiko Saito¹, Toshitaka Baba², Shunsuke Takemura¹, Eiichi Fukuyama¹

1. National Research Institute for Earth Science and Disaster Resilience, 2. Graduate School of Science and Technology, Tokushima University

When observation stations are located apart from an earthquake hypocenter, tsunami arrives much later than seismic waves because tsunami propagates considerably slower than seismic waves. Hence, we effortlessly exclude seismic waves by just setting an appropriate time window when we analyze tsunami signals. However, when analyzing the waveforms recorded inside the focal area, it is difficult to decompose the wavefield into seismic waves and tsunami. We need to employ a theory that describes seismic waves and tsunami simultaneously. For example, Saito and Tsushima (2016) proposed a method for synthesizing ocean-bottom pressure records considering both seismic waves and tsunami. They evaluated the performance of a real-time tsunami forecasting algorithm called tFISH (e.g., Tsushima et al. 2012) by using the synthesized records.

New observation networks such as DONET and S-net are designed for the observation inside the focal area. Therefore, it is fundamentally important to investigate the contributions of seismic waves in tsunami waveforms. Recent development of tsunami observation technology enables us to observe tsunami not only by sea-bottom pressure change but also by sea-surface displacement by using GPS buoys. Inazu et al. (2016) showed that real-time tsunami source estimation is possible if we utilize high-precision, real-time GPS height observations equipped with cargo ships and tankers. At present, a method for synthesizing ocean-surface displacement including both seismic waves and tsunami is urgently required. The present study proposes a method that calculates both the sea surface displacement including seismic waves and tsunami in addition tsunami inundation along coasts. Taking the anticipated Nankai-Trough huge earthquakes as example, we theoretically created the sea-surface displacement waveforms and the inundation. We used the scenarios proposed by Hok et al. (2011) where the earthquake ruptures were simulated based on the friction law established in laboratory experiments and the slip deficit distribution estimated by geodetic-data analysis. By using their rupture scenarios as seismic sources in 3-D seismic-wave propagation simulations, we calculated spatial and temporal variation of the sea-surface displacement field without considering gravity (e.g., Takemura et al. 2016). Then, we included the contribution of gravity to the displacement field (in other words, simulated surface-height propagation as tsunami) by numerically solving nonlinear long-wave tsunami equations. We successfully simulated the inundation process with high-resolution topography data (minimum grid-spacing is ~6 m) by integrating a code referred to as JAGRUS (Baba et al. 2015) to the scheme proposed in this study.

Seismic waves and tsunami simultaneously appeared in the sea-surface displacement during the earthquake rupture, which can be noise for tsunami analyses. The seismic wave contribution to sea-surface displacement was smaller than to the sea-bottom pressure change. Since the moment rate becomes larger when the rupture duration gets shorter, seismic wave contributes more due to shorter rupture duration. On the other hand, tsunami inundation is mainly controlled by the moment but not the moment rate. The data sets created in this study would be useful for practical tests of tsunami-prediction algorithms using sea-surface displacement waveforms.

Keywords: Seismic Wave, Tsunami, Simulation

Observation and simulation of the regional-distance S-PL wave from the very deep ($h=680$ km) Mw 7.9 Ogasawara Islands earthquake of 2015 May 30

*Takashi Furumura¹, Brian L N Kennett²

1. Earthquake Research Institute The University of Tokyo, 2. Research School of Earth Sciences The Australian National University

Deep earthquakes in the subducting Pacific slab frequently produce anomalously large ground motions over Japan along the east coast of Honshu due to an efficient slab waveguide effect for high-frequency ($f > 1$ Hz) signals caused by multiple forward scattering in heterogeneous and high-Q slab.

A recent observation of the Mw 7.9 earthquake beneath the Ogasawara Islands on 2015 May 30 at 680 km depth, produced an anomalously large shock over Japan with a distinctive pattern of ground motion with significantly stretched shaking intensity contours from the hypocenter to northern Honshu along the Pacific seaboard, demonstrated a typical pattern of the deep Pacific slab events.

However, the observed waveforms of regional distances ($D=1000-2000$ km) recorded by the F-net broadband, strong motion instruments indicate that the large ground acceleration arises from relatively low-frequency ($f < 1$ Hz) S-wave pulses and following low-frequency ($f < 0.1$ Hz) signals with long tails. The arrival of the slab-guided high-frequency signal was very late and weak compared with ordinary slab events. Such an anomalous wavefield may arise due to the very great depth of this event, about 100 km deeper than other seismicity in the vicinity.

Numerical simulation of seismic wave propagation employing the 3-D finite-difference method with a detailed structural model of the Pacific slab subduction zone shows how the deep source affects the regional wavefield. The results of the simulation demonstrate that the S waves radiating from the very deep ($h=678$ km) source out of the slab travel upwards and impinge on the crust at around 1000 km epicentral distance with similar slowness to P in the crust to produce strong S-to-P conversions at the free surface. The converted P waves are trapped in the crust with multiple Moho and surface reflections interfering to produce a long-period PL wave. Such a PL wave developed from a very deep source can travel substantial distances with successively supply of S wave from depth to the crustal waveguide for distances to 2000 km. Also the incidence of the S waves with the same slowness as the PL wave traveling in the crust makes a shear-coupled PL (S-PL) wavetrain with long-period ($T=5-10$ s). Later, weak slab-guided S waves from the very deep event are also transferred injected into the crust and continue as an Lg wave traveling in the crustal waveguide.

Though the S-PL wave is often noticed in the teleseismic ($D=50-60$ deg.) records as a dispersed long-period ($T=20-30$ s) wavetrains following the S and SS waves, this study demonstrates that the S-PL wave can be also developed in the regional distances ($D=10-20$ deg.) from very deep sources. However, the visibility of the regional S-PL phases depends strongly on the development of the high-frequency slab-guided waves, which can entirely override the regional seismic wavefield along the slab. The clear observation of the regional S-PL wave from the very deep earthquake beneath Ogasawara Island is because this event occurred out of the main slab.

Keywords: Simulation, 2015 Ogasawara earthquake, SPL wave , Deep-focus earthquake

Cross-Scale Modeling of Great Earthquake Cycles: Methodology, Postseismic Relaxation, Maximum Magnitudes

*Iskander A. Muldashev¹, Stephan V. Sobolev^{1,2}

1. GFZ German Research Centre for Geosciences, Potsdam, Germany, 2. Institute of Earth and Environmental Science, University of Potsdam, Potsdam-Golm, Germany

We present details of a cross-scale thermomechanical model developed with the aim of simulating the entire subduction process from earthquake (1 minute), postseismic processes (minutes to years), seismic cycle and multiple seismic cycles (centures to milleniums) to tectonic evolution at million years' time scale. The model employs elasticity, non-linear transient viscous rheology, and rate-and-state friction. It generates spontaneous earthquake sequences, and, by using an adaptive time-step algorithm, recreates the deformation process as observed naturally over single and multiple seismic cycles.

A developed technique was used to model postseismic relaxation after great subduction earthquakes and for estimation of the maximum magnitudes of the earthquakes in subduction zones.

The set of 2D models is used to study effects of non-linear transient rheology on postseismic processes after great earthquakes. Models predict that viscosity in the mantle wedge drops by 3 to 4 orders of magnitude during the great earthquake with magnitude above 9 due to the power-law creep rheology (major factor) and transient dislocation creep based on experimental data and theoretical mineral physics considerations. This results in significantly different spatial scale and timing of the relaxation processes following the earthquake than it is currently believed. Our model produce large postseismic creep due to visco-elastic relaxation in the mantle wedge that shows up in surface deformation similar to the classical afterslip and therefore can be misinterpreted as an afterslip. The model fits well the GPS data for postseismic slip of Tohoku 2011 earthquake in the time range of 1 day-4 years.

Developed technique is also applied to study key factors controlling maximum magnitudes of earthquakes in subduction zones. Our models demonstrate that maximum magnitudes of the earthquakes are exclusively controlled by the factors that increase rupture width. These factors are: low slab' s dipping angle (the largest effect), low friction coefficient in subduction channel (smaller effect) and high subduction velocity (the smallest effect). In agreement with observations, our models also suggest that the largest earthquakes should occur in subduction zones with neutral (most frequently) or moderately compressive deformation regimes of the upper plate. This is a consequence of the low dipping angles and low static friction coefficients in the subduction zones with largest earthquakes, rather than a reason for the largest earthquakes. The predicted maximum magnitudes for the subduction zones of different geometries are consistent with the observed magnitudes for all events.

Keywords: earthquake modeling, seismic cycle, postseismic relaxation, great earthquakes, maximum magnitude

Numerical simulation of the drag force from the mantle convection on the deformation pattern of the northeastern margin of the Tibetan Plateau

*Aiyu Zhu¹

1. Institute of Geophysics, China Earthquake Administration

Based on the recent observation and research results, including lithosphere velocity, rheological structure and crustal deformation, we established a 3D finite element model of the northeastern Qinghai Tibet Plateau, in which, the control effect, consist of the plateau gravity, block horizontal interaction, the main active fault, drag force from the mantle convection and some other internal and external conditions are considered. The simulation results are shown as follows: Continuous deformation is the main characteristic of current tectonic activity in northeastern margin of the Tibetan Plateau; Block horizontal interaction, plateau accumulated gravity, especially small-scale mantle convection drag force have important influence on the characteristics of surface deformation; Taking into account the view of the coupling of lithosphere / asthenosphere and decoupling of upper mantle, we put forward the rheological experiment on rock mechanical properties of the upper mantle decoupling mechanism, considering intensity factor ratio and coefficient of viscosity, we find that the simulation results is well agree with observation of GPS. The simulation results further support coupling mechanism of the northeastern margin of the Qinghai Tibet Plateau deformation; meanwhile, the calculation method of the mantle convection drag force is proposed, i.e., Transverse inhomogeneity of rheological properties of lithosphere at different block should be taken account in the calculation.

Keywords: northeastern margin of the Tibetan Plateau, the mantle convection drag force, Numerical simulation

Influence of fault surface condition on slip stability in large-scale biaxial friction experiment

*Futoshi Yamashita¹, Eiichi Fukuyama¹, Shiqing Xu¹, Hironori Kawakata², Kazuo Mizoguchi³, Shigeru Takizawa¹

1. National Research Institute for Earth Science and Disaster Resilience, 2. Ritsumeikan University, 3. Central Research Institute of Electric Power Industry

Slow slips and/or foreshocks preceding large earthquakes were often observed (e.g. Bouchon *et al.*, 2011; Kato *et al.*, 2012). To reproduce and investigate those activities in laboratory, we have conducted stick-slip experiments using large-scale biaxial friction apparatus at NIED (Fukuyama *et al.*, 2014). We used two rectangular metagabbro blocks as experimental specimen. The nominal contacting area was 1.5 m long and 0.1 m wide and the contacting surfaces were polished so that the undulation was less than 10 μm before the first experiment. We repeatedly conducted the experiments with the same pair of specimens, which means the fault surface continuously evolved with the frictional slip. The stick-slip experiments were conducted under the condition of constant normal stress of 6.7 MPa and loading rate of 0.01 mm/s. To monitor various phenomena on the fault, we installed dense arrays of strain gauges and PZT seismic sensors along the fault. In the first experiment, very few foreshocks were observed over the entire history of the experiment while precursory slow slips were observed before each main stick-slip event. We also found that both the occurrence location of slow slip and its occurrence time relative to the main rupture followed a mono-modal distribution at this initial stage. In later experiments, however, a variety of occurrence times and locations of slow slips was observed. The number of foreshocks also increased with the evolution of the fault surface, and the estimated hypocenters were located around the area where many gouge particles were generated during those experiments. To further investigate the relationship between foreshock activities and the existence of gouge, we focused on two experiments at the similar evolution stage but with different initial gouge conditions; one experiment was started with all previous gouge removed while the other was started with gouge from the previous experiment remained. Note that distribution of the gouge is not homogeneous but heterogeneous, because we did not give any operations to make the gouge layer uniform. First of all, both the number and magnitude of foreshocks were larger in the experiment with pre-existing gouge (denoted by PEG hereafter). In particular, relatively large number of big foreshocks were observed, which was revealed by a lower b value relative to the other. We also found that the maximum magnitudes of the foreshocks increased with the slip distance during the experiment without PEG, whereas they are almost constant in the experiment with PEG. The increase in the foreshock magnitude should be caused by an increase in the amount of newly generated gouge with slip. Therefore, these observations suggest that the upper limit of the foreshock magnitude is controlled by the gouge layer thickness. The gouge condition also affects how main event occurs. In the experiment without PEG, precursory slow slips were observed before every main event but foreshocks occurred only at the end of the nucleation process. The strain data suggested that foreshock occurrence in this condition requires relatively large stress concentration and subsequent stress release induced by the slow slip. In the experiment with PEG, on the contrary, no clear precursory slow slips were observed by the strain measurement. Instead, the number and magnitude of foreshocks increased towards the main event at an accelerated rate, which were confirmed by a decreasing b value. Spatiotemporal distribution of foreshock hypocenters suggests that foreshocks migrate and cascade up to the main event. We infer that heterogeneous gouge distribution caused stress-concentrated and destructive patches, which impeded slow and stable slip and activated foreshocks on the fault. These results confirm that fault surface condition affects the slip stability on it even under the same loading condition. They also suggest

that b value is a key parameter to explore the condition.

Keywords: Friction experiment, Slow slip, Foreshock, b value, Heterogeneity, Gouge

O(N) methods for spatiotemporal BIEM

*Daisuke Sato¹, Ryosuke Ando¹

1. Graduate School of Science, University of Tokyo

Recent progressions of seismic inversions has shown off the numerous results which cannot be explained by the ordinary source modelings, as seen in Tohoku 2011 and Kumamoto 2016. Particularly, the hierarchical features of fault sources have been clearly detected, e.g. hierarchical asperity distribution of Tohoku-Oki [Ide Aochi 2013] and the scaling of critical slip distance [Mikumo et al. 2003]. To get the whole descriptions, i.e. the theory of earthquakes, we must exceedingly develop the source modelings including those hierarchical behaviors.

The disturbance is the numerical cost. Boundary integral equation method (BIEM) has been widely used for the source modelings to resolve the highly nonlinear boundary conditions of the fault, but it is quite time-consuming method [Ando 2016]. The original BIEM needs the cost $O(N^2L)$ (N : fault unit number, L fault length). For example, to resolve M4 (km) events on the M9 fault (400km), we need a Peta-scale simulator! Our aim is $O(N)$ (theoretical fastest) algorithm to solve this problematic situation. We combine the fast domain partitioning method (FDPM)[Ando et al. 2009, Ando2016] and H-matrix method, then construct $O(N)$ method for hyperbolic equations (FDPM=H-matrix). Furthermore, this $O(N)$ method is principally faster than the corresponding finite element modelings.

In the presentation, we talk about how to apply the H-matrix method to elastic equations and the performance evaluations of the implemented algorithm. (i) How to achieve $O(N)$; The elastic equations have the singular wave front, thus it is known that the naive applications of H-matrix method cannot achieve $O(N)$ [Yoshikawa and Yamamoto 2015]. FDPM provides the key idea to solve this problem. The implementation is based on the physical fact that the kernel is regular along the ray, although the kernel is singular across the ray [Aki and Richards 1980]. Thus we can safely apply the H-matrix method if we can define the ray coordinate on the kernels. This abstract idea can be mostly implemented by the Adaptive cross approximations on Front domain (Domain F in the terminology of [Ando 2016]) and Tensor Cross Approximations on Near-field and Static regions (Domain I and S). Some approximations of causality is also required and we clear the problem analytically. (ii) Performance evaluations; We show the accuracy and cost of the proposed algorithm based on some case studies. FDPM=H-matrix has some crucial approximations of time-directions, thus we carefully review it and discuss the accuracy. The accuracy is quite good (with 0.3 percent error in some cases) if we sufficiently resolve the dynamic rupture. However, because of the causality conditions, $O(N)$ looks not to be achieved rigorously in some cases and the cost reduction looks to draw back to $O(N^{1.5})$, thus we also discuss the alternative approximations to achieve $O(N)$ even in these situations. The result of cost reduction is also discussed in the presentation.

If we use this FDP=H-matrix method, we can extensively study the complex fault modelings and examine the theoretical hypothesis of the source parameters as already referred. Because of the numerical costs, nonplanar features of faults(for example, damage zones, branchings and fractal fault roughness) are not so studied in the current stages compared with planar fault modelings. Those features are crucially related to the source parameters [Andrews 1976], thus this method will finally contributes to the study of observed source parameters of faults.

Keywords: Spatiotemporal BIEM, $O(N)$ method, Dynamic Rupture of Faults, H-matrix

Renormalized source parameters on fractally rough faults

*Daisuke Sato¹, Ryosuke Ando¹

1. Graduate School of Science, University of Tokyo

Nonplanar properties of faults are considered to contribute to the fault source parameters [Andrews 1976, Scholz 2002]. However it is poorly studied compared to the comprehensive studies of planar fault models [Ando Yamashita 2007]. Partial reason is that the numerical cost of nonplanar faults is quite higher than the planar modelings. We proposed the $O(N)$ method (FDP=H-matrix) in another presentation and solved this cost problem. So, we study the nonplanar effect of the fault using this method and report the result. We mainly focus on the fractal fault roughness universally observed in natural faults [Scholz 2002, Renard et al 2013].

The effect of the roughness is studied experimentally [Ohnaka 2002] and theoretically [Gold'stein and Mosolov 1991, Horvath Herrmann 1992], but those conclusions do not coincide with each other. The effect of fault roughness is well studied by the experiment of [Ohnaka 2002] and he found the critical slip scaling distance (D_c) linearly depends on the lower cutoff wavelength of the fractal scaling. This D_c scaling is consistent with the expected behavior of fault [Ide Aochi 2013]. However, the past renormalization group approach of the fractal fault predicted the different scaling of D_c [Gold'stein and Mosolov 1991]. The scaling exponent is smaller than the 0.5 (roughly 0.23 if we use the observed Hurst exponent 0.77 [Renard et al. 2013]) and quite weaker than the linear dependence as observed in experiments. Also, some theory asserts that terminal velocity becomes slower and slower if the earthquake becomes large [Horvath Herrmann 1992] but this prediction is inconsistent with the experiment [Ohnaka 2002] and simulations [Ide Aochi 2004, Dunham et al. 2011] It asserts the discrepancy of the interpretation from the actual physics behind the experiment and the lack of the theory. However, the studied parameter is still limited and the system size is not so large to discuss those scaling behavior.

Therefore, we present some results on dynamic rupture simulations on fractal rough faults using $O(N)$ method. The current result is as follows. Dynamic rupture apparently propagates at sub-shear velocity but looks not so slower than the theoretical prediction; In some parameters where the crack with slip weakening friction does not stop spontaneously, we observed the subshear velocity of crack propagations. However, the terminal velocity looks faster than the theoretical prediction. Therefore, we constructed the estimation of the terminal velocity for the case where the Griffith energy becomes linearly depends on the crack sizes. This estimation predicts the the sub-shear terminal velocity. It looks consistent with our result and [Ide Aochi 2013]. The result of D_c scaling will be also discussed in the presentation.

Keywords: Rough Faults/ fractal roughness, source parameters, Dynamic Rupture of Faults

Dynamic rupture simulation for seismic hazard assessment: Application to the Yamazaki fault zone, central Japan

*Yuko Kase¹, Kohei Abe², Atsushi Miwa², Hideki Kosaka³

1. Geological Survey of Japan, AIST, 2. Oyo Corporation, 3. Kankyo Chishitsu Company Limited

In seismic hazard assessment, many earthquake rupture scenarios need to be weighted. For these scenarios, rupture area is one of the important factors, but the evaluation of the rupture area is unfortunately difficult before event. On the other hand, dynamic rupture simulations can calculate physically reasonable rupture processes based on fault geometries, stress conditions, and frictional constitutive laws. We propose dynamic rupture modeling for weighting of earthquake rupture scenarios, and apply the modeling to the Yamazaki fault zone, central Japan.

The Yamazaki fault zone is left-lateral strike-slip active fault in central Japan. We model three faults, the Ohara, Hijima, and Yasutomi faults in the northwestern part of the Yamazaki fault zone as a continuous vertical fault plane about 50 km long with surface rupture, based on the fault traces. The fault model is combined with assumption of stress field. Principal stresses are proportional to depth, based on the borehole data (Yamashita et al, 2004). A stress inversion result shows that the azimuth of the maximum principal stress is from N60°E to N100°E. We calculate dynamic rupture processes, using a finite-difference method (Kase and Day, 2006), to search the azimuth of the maximum principal stress and frictional coefficients most consistent with an observed left-lateral dislocation of about 2 m on the surface (Okayama Prefecture, 1996).

We simulate a variety of rupture processes on the Yamazaki fault zone, depending on parameters, but the simulation results show some characteristic rupture processes. For example, when the coefficients of friction are the same on the three faults, a rupture initiating on the Ohara fault propagates to the Hijima fault, but it terminates in the boundary between the Hijima and Yasutomi faults because of negative stress drop. When the coefficients of friction of the Yasutomi fault are less than those of the other faults, on the other hand, the rupture initiating on the Ohara fault propagates to both of the Hijima and Yasutomi faults, but the deep portion of the Yasutomi fault remains unrupture. These characteristics of rupture process can be useful information for weighting of earthquake rupture scenarios.

Keywords: dynamic rupture, Yamazaki fault, numerical simulation, seismic hazard assessment

MODELLING OF NEAR-FAULT EARTHQUAKE GROUND MOTION WITH EARTHQUAKE SIMULATIONS

*Aydin Mert¹

1. Kandilli Observatory and Earthquake Research Institute

Engineering structures are usually designed on the base of accelerations derived from ordinary Probabilistic Seismic Hazard Analysis (PSHA) under the hypothesis of far-field conditions and further modified taking into account the local seismic response. As a consequence, a structure might not have proper safety levels if it is located close to an earthquake source. Despite the progress that has been accomplished so far by seismologist and earthquake engineers, the conducted research and papers in the literature highlighted that there could be a deficiency of seismic safety in near-field domains if the near-field seismic effects are not considered in the seismic design, as is the case of the Turkish seismic code.

The main purpose of this study is to analyze the near-field effects, focusing to evaluate ground shaking for specific fault configurations, specific source parameters and rupture process. For this reason, scenario simulations will be performed systematically to investigate the influence of different source parameters on the resulting near-source ground motion and to quantify the uncertainty in the employed source parameters and the associated variability in ground motion. The basis of the methodology is to generate a suite of synthesized seismograms from quasi-dynamic rupture models that use measurable or theoretically determined physical parameters that define fault rupture and control resulting ground motion.

Recent, well-instrumented earthquakes generated a large number of ground-motion recordings from sites close to the active fault. In these datasets, the observed variability of seismic ground motion meaningfully different from those far from the source not only in terms of intensity but also in terms of nature and topology. This contribution of earthquake source complexity to the ground-motion variability is generally thought to be significant, especially in the area near seismic sources. Only a few studies systematically investigated the influence of different source parameters on the resulting near-source ground motion. For that reason, there is a clear need to develop reliable synthetic ground motions or simulations reveal that not only influence of different source parameters on the resulting near-source ground motion but also capture different physical characteristic of near fields records both qualitatively and quantitatively.

Keywords: NEAR-FAULT EARTHQUAKE GROUND MOTION, EARTHQUAKE SOURCE PARAMETERS, SIMULATION OF STRONG GROUND MOTION, GREEN' S FUNCTIONS

Rupture process of the 2016 Meinong, Taiwan, earthquake and its effects on strong ground motions

*Hongqi Diao¹, Hiroaki Kobayashi¹, Kazuki Koketsu¹

1. Earthquake Research Institute, University of Tokyo

Meinong Taiwan earthquake occurred in the Meinong area of southern Taiwan on 6 Feb. 2016, but caused the most severe damages in Tainan. Large amplitude accelerations and velocity pulses in both EW direction and NS direction were recorded by strong motion stations in Tainan. To investigate the characteristics of strong motion distribution in Tainan, a joint source inversion was performed. The results of source process show that the rupture propagated from hypocenter toward northwest nearly along strike direction with a constant velocity close to shear wave velocity; the main rupture area occurred in the northwest of hypocenter and was close to Tainan; the radiation pattern of S waves generated from the main rupture area, which is dominated by oblique slips with large rake angle and small dip angle of faulting, and the small azimuth between rupture propagation direction and the direction of seismic ray, contributed jointly to the directivity effect observed in Tainan. Velocity pulses, having larger components along strike parallel direction than that along strike normal direction, recorded in Tainan during Meinong event, have important implications on the seismic design of tall buildings in near fault region.

Keywords: rupture process, rupture directivity effect

Super-shear fault rupture propagation during the 2016 Kumamoto earthquake (Mw7.1); Numerical tests and resolution

*Nelson Pulido¹

1. National Research Institute for Earth Science and Disaster Resilience

I investigated the rupture process of the April 16, 2016 Kumamoto earthquake, using a seismic back-projection methodology (Pulido et al. 2008, Pulido 2016), and a dense array of near-source strong motion records from the K-NET/KiKnet networks. The main target of this study is to understand the evolution of the rupture velocity during fault rupture propagation. I selected all the KNET/KiKnet records of the mainshock within 100 km around the Hinet epicenter (112 stations), and used the fault-parallel component rotated from the horizontal components. I bandpass filtered the data between 5 to 10 Hz and calculated the envelopes of velocity time series. Envelopes were stacked within a horizontal grid mesh covering the regions around the Hinagu and Futagawa fault traces and beyond, to obtain a temporal and spatial image of rupture propagation. My back-projection results show that significant grid energy was released in a region spanning 43km length along the Hinagu (16km) and Futagawa (27 km) fault zones. Back-projection results show a bilateral fault rupture propagation along the Hinagu and Futagawa faults, characterized by a slow sub-Rayleigh rupture velocity of 1.4 ~ 1.7 km/s, for the first 5.5 seconds of imaged rupture (4~9.5s from the origin time, OT). The rupture propagation towards the NE (along the Futagawa fault) experienced a very rapid increase in rupture velocity by reaching a value ~1.4 times larger than the average S-wave velocity ($V_{rup} = 4.7$ km/s) at 9.5s from OT, and remained super-shear for approximately 4.5 s (9.5 ~14s from OT) until fault rupture arrest. I also imaged a clear sub-Rayleigh rupture propagation towards the SW along the Hinagu fault zone ($V_{rup} = 3.1$ km/s), from 11 to 14 seconds after OT. I performed several numerical tests to analyze the effect of station distribution and the ability of my back-projection method to resolve the rupture process. I also performed multiple tests using actual records of aftershocks of the Kumamoto earthquake to test the accuracy of my results. All these tests indicate that the super-shear rupture propagation during the Kumamoto mainshock is a robust feature of my imaging results.

Keywords: 2016 Kumamoto earthquake, super-shear fault rupture, strong ground motion, seismic back-projection

The cause of long-time-duration long-period ground motion observed in Hokkaido during off-Tohoku earthquakes

*Shinako Noguchi¹, Takuto Maeda², Takashi Furumura²

1. Association for the Development of Earthquake Prediction, 2. The University of Tokyo

We found a development of anomalously large and long-time-lasting long-period ground motions in the area around Ishikari, Hokkaido Japan, during off-Tohoku earthquakes. In order to clarify the generation mechanism of this anomalous wave, we conducted a set of numerical simulations of seismic wave propagation in realistic 3D heterogeneous subsurface structures by means of a finite difference method (FDM).

The anomalous long-period wave spreads Ishikari Basin and Teshio Basin, Hokkaido, was clearly observed for shallow earthquakes occurred off-Tohoku. The dense broadband records of Hi-net short-period seismographs after correcting the instrumental response showed that a large long-period ground motion ($T=14\sim 18$ s) lasting more than 200 s appears in the region in Hokkaido. This long-period ground motion dominates in both horizontal and vertical components indicating dominance of surface waves propagating northward. Such anomalous wave did not appear obviously during the earthquakes away from the off-Tohoku region.

Based on the geophysical reflection and refraction experiments and analysis of the gravity data, it is known that deep (~ 10 km) tectonic basins extend from northern Hokkaido to the sea of southern Hokkaido toward the direction to off-Tohoku through the west of Hidaka Mountains. Thus, it is expected that such deep basin structure causes strong effect on the development of the anomalous long-period ground motions mentioned above.

To investigate the cause of the observed long-time-lasting long-period ground motions with interaction to the heterogeneous subsurface structure below Hokkaido in detail, we conducted a FDM simulation of seismic wave propagation using the OpenSWPC (Maeda et al., 2017). We used a realistic 3D subsurface structure model including topography, seawater, sediments and subducting Pacific plate. The result of the simulation demonstrated the development of the long-period ground motion in the area around Ishikari Basin and Teshio Basin which qualitatively reproduces the observed feature, however the duration of the simulated long-period ground motion was not long enough compared with the observation. By modifying the sedimentary structure where the P- and S-wavespeed of the sedimentary layers were replaced with much smaller values, we succeeded in obtaining much longer-time lasting long-period ground motions similar to the observation. The results of the simulation with snapshots of seismic wavefield at each time step and movies demonstrating clearly the process in which the surface waves generated above the epicenter were trapped and amplified in deep sediments at south off Hokkaido, and radiated the long-period motion to northward for a long time to develop a large and long-time-lasting long-period ground motion.

Keywords: Long-period ground motion, Numerical simulation, Surface wave, Long-time duration, Deep basin

Regional earthquake induction around the Korean Peninsula after the 2011 M9.0 Tohoku-Oki megathrust earthquake

*Tae-Kyung Hong¹, Junhyung Kim¹, Seongjun Park¹

1. Department of Earth System Sciences, Yonsei University

Megathrust earthquakes produce large permanent lithospheric displacements as well as strong transient ground shaking up to regional distances. The lateral permanent displacements construct stress shadows in a wide backarc region. The Korean Peninsula is placed in the far-eastern Eurasian plate that belongs to a stable intraplate region with a low earthquake occurrence rate and diffused seismicity, and is located in the backarc at ~1300 km in the west from the epicenter of the 11 March 2011 M9.0 Tohoku-Oki earthquake. The seismicity around the Korean Peninsula was increased significantly after the 2011 M9.0 Tohoku-Oki earthquake. Strong seismic waves cause large dynamic stress changes, incurring fluid migration and increasing pore fluid pressure in the media. The lithospheric displacements directing to the epicenter on the convergent plate boundary develop transient radial tension field over the backarc lithospheres. The seismic velocities in the lithosphere changed abruptly up to 2 % after the megathrust earthquake, which recovered gradually with time for several years. A series of moderate-sized earthquakes and earthquake swarms occur as a consequence of medium response to the temporal evolution of stress field. In particular, two strike-slip earthquakes with magnitudes of M_L 5.1 and 5.8 occurred in the southeastern Korean Peninsula on September 12, 2016. The two events occurred within 48 minutes. The M_L 5.8 earthquake was the largest event in the Korean Peninsula since 1978 when national seismic monitoring began. More than 500 aftershocks with local magnitudes greater than or equal to 1.5 followed the events for two months. The long-term evolution of seismicity is expected to continue until the ambient stress field is fully recovered.

Recurrence Pattern of Tsunami events of Nankai Earthquake recorded in lacustrine sediments along the eastern coast of the Kii Peninsula, southwest Japan.

*Hiromi Matsuoka¹, Makoto Okamura¹, Mitsuo Tsuzuki², Hiroaki Uratani²

1. Kochi University, 2. Disaster Mitigation Research Center, Nagoya University

We studied on tsunami sediment in small lakes along the Nankai Trough for the reconstruction of prehistoric tsunami. Total 33 cores were collected from the three lakes named Ashihama-ike, Zasa-ike and Usuzuki-ike, which located on behind coastal ridge along the southeastern coast of Kii Peninsula. These lakes preserved last 3500 years record of Nankai Earthquake tsunamis. Tsunami events are observed intervals of 3500-3000 yBP, 2700-2000 yBP and 1300-1000 yBP. Furthermore, each interval is composed 2-3 events that decrease in size. These recurrence mode of tsunami events indicate fractal-like patterns.

Keywords: Nankai Earthquakes, tsunami sediments, recurrence pattern